

# Interactive Control over Temporal Consistency while Stylizing Video Streams

Sumit Shekhar<sup>1\*</sup> , Max Reimann<sup>1\*</sup> , Moritz Hilscher<sup>1</sup>, Amir Semmo<sup>1,2</sup> , Jürgen Döllner<sup>1</sup>, and Matthias Trapp<sup>1</sup> 

<sup>1</sup>Hasso Plattner Institute for Digital Engineering, University of Potsdam, Germany

<sup>2</sup>Digital Masterpieces GmbH, Germany  
("\*" denotes equal contribution)

## Abstract

With the advent of Neural Style Transfer (NST), stylizing an image has become quite popular. A convenient way for extending stylization techniques to videos is by applying them on a per-frame basis. However, such per-frame application usually lacks temporal consistency expressed by undesirable flickering artifacts. Most of the existing approaches for enforcing temporal consistency suffers from one or more of the following drawbacks: They (1) are only suitable for a limited range of techniques, (2) typically do not support live processing as they require the complete video as input, (3) cannot provide consistency for the task of stylization, or (4) do not provide interactive consistency-control. Note that existing consistent video-filtering approaches aim to completely remove flickering artifacts and thus do not respect any specific consistency-control aspect. For stylization tasks, however, consistency-control is an essential requirement where a certain amount of flickering can add to the artistic look and feel. Moreover, making this control interactive is paramount from a usability perspective. To achieve the above requirements, we propose an approach that can stylize video streams while providing interactive consistency-control. For achieving interactive performance, we develop a lite optical-flow network that operates at 80 Frames per second (FPS) on desktop systems with sufficient accuracy. Further, we employ an adaptive combination of local and global consistent features and enable interactive selection between the two. By objective and subjective evaluation, we show that our method is superior to state-of-the-art approaches.

## CCS Concepts

- Computing methodologies , . . . , *Image-based rendering; Non-photorealistic rendering; Image processing*

## 1. Introduction

For thousands of years, paintings have served as a tool for visual communication and expression. However, it was not until the late 20<sup>th</sup> century that computers were used to simulate paintings [Hae90]. In the course of following decades, the field of artistic stylization [KCWI13] has significantly developed and extended by NSTs [SID17, JYF\*20]. Even though a large number of image stylization techniques exist, extending these to video remains challenging. A major obstacle in this regard is the enforcement of temporal coherence between stylized video frames. With the proliferation of video streaming applications, stylizing video streams has become popular, however, the requirements of low-latency processing add additional challenges. Most of the existing methods, to address the above, can be classified into one of the following four categories:

**Style Specific.** A common approach is to develop a specific method for a particular artistic style and exploit its characteristics for temporal coherency [BNTS07]. Such methods work effectively for the specific target style, however, do not generalize

well. Many of these specialized approaches have been discussed by Bénard *et al.* [BTC13].

**Coherent Noise.** Another class of techniques adopt and transform a generic, temporally-coherent noise function to yield a visually plausible stylized output [BLV\*10, KP11]. Compared to target-based coherence enforcement [BNTS07], these are applicable to a wider range of techniques but are limited for scenarios with rapid temporal changes.

**Stylization by Example.** More recently, authors have adopted a stylization-by-example approach to support a wide range of stylization techniques [BCK\*13, JST\*19, TFK\*20, FKL\*21]. However, this approach requires the paring of the complete video and keyframe marking. Thus, by design it is not applicable to video streams.

**Consistent Video Filtering.** One can also enable stylization of video streams using consistent video filtering techniques. Existing approaches are either not well-suited for Image-based Artistic Rendering (IB-AR) [BTS\*15, YCC17] (Fig. 1) or do not provide interactive consistency control [LHW\*18, TDKP21], which

Table 1: Comparing existing consistent video filtering methods with ours with regards to consistency-control. Here, the color **green** denotes the aspect which is favourable to interactive consistency-control while the color **red** denotes otherwise (“NA” stands for Not-Applicable).

	Bonneel <i>et al.</i> [BTS*15]	Yao <i>et al.</i> [YCC17]	Lai <i>et al.</i> [LHW*18]	Shekhar <i>et al.</i> [SST*19]	Thiemonier <i>et al.</i> [TDKP21]	Ours
Requires pre-processing?	No	Yes	No	Yes	No	No
Provides consistency-control at inference time?	Yes	No	No	Yes	No	Yes
Is the consistency-control interactive?	No	NA	NA	Yes	NA	Yes

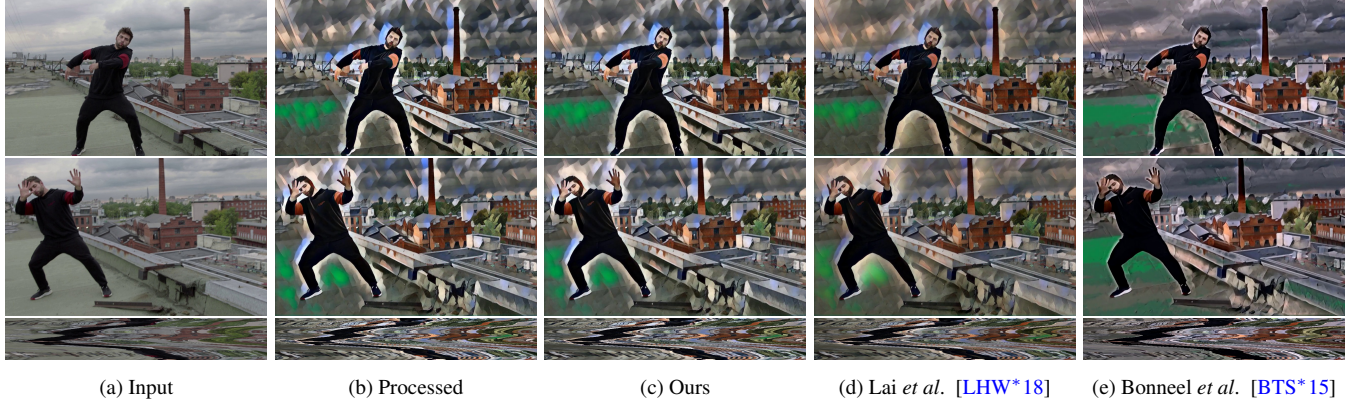


Figure 1: For the top-row: first two columns depicts (a) input and (b) processed result for frame-24, column three to five depict the corresponding consistent output using (c) Ours (d) Lai’s, and (e) Bonneel’s method. For the mid-row: depict the corresponding results for frame-80. For the bottom-row: we show the Temporal Slice Image (TSI) for the entire video sequence depicting long-term temporal similarity with the per-frame processed output. Note, that our method is able to preserve the look and feel of the per-frame processed result in comparison to the method of Lai *et al.* which suffers from color bleeding artifacts while the stylized textures are lost for the output of Bonneel *et al.*. Please see the supplementary material for video results.

is an essential requirement for artistic rendering [FLJ\*14]. Currently, the only method that provides interactive consistency-control is limited to offline processing and requires pre-processing [SST\*19].

We aim to develop a temporal-consistency enforcement approach for artistic stylization techniques that provides (1) interactive consistency-control and (2) online processing to facilitate the application to video streams.

A determining factor towards the slow performance of existing online and interactive consistent video filtering technique [BTS\*15] is the costly step of optic-flow computation. Previous works using learning-based methods are able to achieve a considerable accuracy for optic-flow estimation [TD20, JCL\*21]. However, we argue that such a high accuracy is not particularly necessary to enforce temporal consistency for artistic stylization tasks. To validate our conjecture, we conduct a user study, wherein the participants prefer the final consistent video output generated using our flow network as compared to that being obtained using State-of-the-art (SOTA) approaches. We define artistic stylization as the adaptation of colors, textures, and strokes. While our approach is effective for most image-based stylization techniques (e.g., NSTs, algorithmic filtering), it is not able to handle significant shape or content inconsistencies between frames introduced by semantically-driven image synthesis (e.g., image-to-image diffusion-based models [RBL\*22]), as flow-based warping is insufficient to enforce consistency in these cases.

In contrast to accuracy, little attention has been paid to improve

the run-time performance of optic-flow estimation, but which is essential for online-interactive editing. To this end, we develop a lite optic-flow neural network that runs at a high-speed (approx. 80 FPS on mid-tier desktop GPUs) while maintaining sufficient accuracy. The compact network is also deployable on mobile devices (iPhones and iPads) where it runs at interactive frame rates (24 FPS on iPad Pro 2020). We use the optic-flow output from the above network to enforce warping-based consistency at interactive frame rates. Moreover, we construct an adaptive consistency prior which allows for global and local temporal-consistency control. To summarize we present the following contributions:

1. A novel approach for making per-frame stylized videos temporally consistent via adaptive combination of local and global consistency features which allows for interactive consistency-control.
2. A lite optic-flow network, to achieve interactive performance, that runs at 80 FPS on a mid-tier desktop PC and at 24 FPS on a mobile device while achieving reasonable accuracy.

## 2. Background & Related Work

**Consistent Video Filtering.** Lang *et al.* [LWA\*12] propose a solution to enforce temporal consistency for a large-class of optimization-based problems via iterative filtering along the motion path. Dong *et al.* [DBZY15] address the problem of temporal inconsistency for enhancement algorithms by dividing individual video frames into multiple regions and performing a region-based spatio-temporal optimization. Bonneel *et al.* [BTS\*15] was the

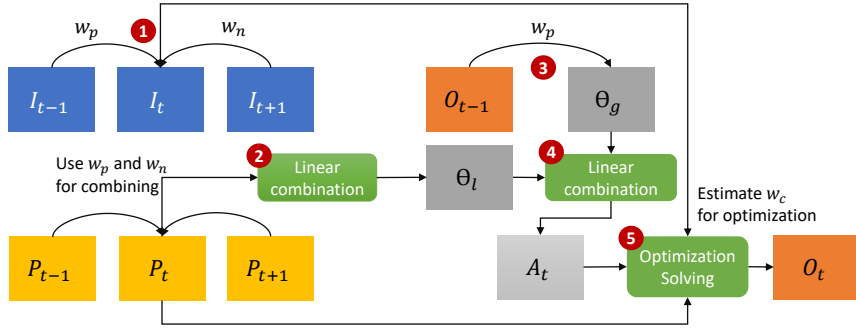


Figure 2: Schematic overview of our approach: (1) We start by calculating the warping weights  $w_p$  and  $w_n$  using Eqn. 3. (2) The computed weights are used to linearly combine  $P_t$ ,  $P_{t-1}$ , and  $P_{t+1}$  to obtain the locally consistent image  $L_t$ , see Eqn. 2. (3) To obtain the globally consistent version  $G_t$  we warp the output at previous time instance  $O_{t-1}$  as depicted in Eqn. 4. (4) The local and global consistent images,  $L_t$  and  $G_t$ , are linearly combined to obtain a temporally smooth version  $A_t$ , see Eqn. 5. (5) To include high-frequency details from the per-frame processed result,  $A_t$  and  $P_t$  is adaptively combined via the optimization in Eqn. 1 using the weights  $w_c$  (Eqn. 7) to obtain the final result  $O_t$ .

first to present a generalized approach for consistent video filtering which is agnostic to the type of filtering applied on individual video-frames. The method combines gradient-based characteristics of the per-frame processed result with the warped version of the previous-frame output using a gradient-domain based optimization scheme. Yao *et al.* [YCC17] propose a similar approach however considers multiple key-frames for warping-based consistency to avoid problems due to occlusion. Both of the approaches assume that the gradient of the processed video is similar to that of the input video and thus cannot handle artistic rendering tasks where new gradients resembling brush strokes are generated as part of the stylization process. Moreover, due to slow optic-flow computation they are non-interactive in nature. Shekhar *et al.* [SST\*19] employs a similar formulation as Bonneel *et al.*, with the difference of using a temporally denoised version of the current-frame for consistency guidance. However, the temporal denoising requires the complete video as input making the method offline in nature. Lai *et al.* [LHW\*18] propose the first learning-based technique in this context. The authors employ perceptual loss to enforce similarity with the processed frames and for consistency make use of short-term and long-term temporal losses. Thimonier *et al.* [TDKP21] employ a ping-pong loss and a corresponding training procedure for temporal consistency. Both the learning based technique are faster than their optimization-based counterpart since they do not perform optic-flow computation at test time. However, these learning based techniques do not allow to control the degree of consistency in the final output which is vital for the task of stylization. Thus, the above discussed methods are either non-interactive/offline or do not provide any consistency control at inference time. Our approach addresses these limitations (Tab. 1).

**Optic Flow for Consistent Filtering.** Both Bonneel *et al.* and Yao *et al.* use the PatchMatch algorithm [BSFG09] for flow-based warping, however, the slow performance of PatchMatch makes them non-interactive. Lai *et al.* use FlowNet 2.0 [IMS\*17] for flow-based warping to design their short-term and long-term temporal consistency losses. FlowNet 2.0 is on par with the quality of state-of-the-art classical methods, however, due to large number of pa-

rameters and operations, achieves only interactive frame rates even on high-end desktop Graphical Processing Units (GPUs). An improved compact optic-flow Convolutional Neural Network (CNN) is proposed by Sun *et al.* [SYLK18] – PWC-Net. It combines coarse-to-fine estimation with pyramidal image features, correlation, warping, and CNN-based estimation. Furthermore, a refinement CNN is stacked at the end to improve the final flow estimate. PWC-Net is orders of magnitude smaller than FlowNet 2.0, runs at real-time frame rates using desktop GPUs. Liu *et al.* [LZH\*20] employ their approach to train a similar architecture in an unsupervised setting and achieve reasonable accuracy – ARFlow. LiteFlowNet and its successor LiteFlowNet2, both proposed by Hui *et al.* [HTL18, HTL20], have similar compact architectures. Further improvement in accuracy is achieved by models using iterative refinement, such as RAFT [TD20] and transformer modules such as GMA [JCL\*21], however they heavily trade runtime for accuracy. Based on a runtime-accuracy comparison (see Sec. 3.2), we select PWC-Net as a base network to develop a "Lite" flow network with improved performance for interactive consistent filtering.

**Temporal Consistency for Video Stylization.** Litwinowicz [Li97] describes a technique to apply an impressionist effect on images and videos. For enforcing temporal coherence, optical flow was used to transform the brush strokes from one frame to the next. Winnemöller *et al.* [WOG06] develop a real-time video and image abstraction framework. The authors employ soft quantization that spreads over a larger area, thus significantly reducing temporal incoherence. Bousseau *et al.* [BNTS07] advects texture in forward and backward direction using optical flow for coherent water-colorization of videos. Numerous such specialized video-based approaches have been discussed by Bénard *et al.* [BTC13]. The above classical IB-AR techniques approximate rendering primitives by modifying traditional image filters. Most often, they use low-level image features for modeling and fail to model structures resembling a particular style. Recently, deep CNNs were successfully used to transfer high-level style attributes from a painting onto a given image [GEB16]. Various methods have been proposed to extend the above for videos [HWL\*17, CLY\*17, GJAF17, RDB18, LLKY19, PP19, DTD\*21]. Ruder *et al.* [RDB18]

propose novel initialization technique and loss functions for consistent stylized output even in cases with large motion and strong occlusion. The methods of Gupta *et al.* [GJAF17], Chen *et al.* [CLY\*17], and Huang *et al.* [HWL\*17] enforce consistency via certain formulation of temporal loss and use optical flow based warping only during the training phase thus achieving fast performance. Puy and Pérez [PP19] develop a flexible deep CNN for controllable artistic style transfer that allows for addition of a temporal regularizer at testing time to remove the flickering artefacts. The above method comes closest in terms of providing some consistency control at test time for NST-based methods. However, they cannot handle classical stylization techniques. Stylization by example [BCK\*13, JST\*19, TFK\*20, FKL\*21] caters to both (classical and neural) paradigms via priors involving keyframe-based warping but can only be applied as an offline process. We aim to propose a generic solution which is agnostic to the type of stylization and provides online performance and interactive consistency-control.

### 3. Method

#### 3.1. Temporal Consistency Enforcement

Given an input video stream  $\dots, I_{t-1}, I_t, I_{t+1}, \dots$  and its per-frame processed version  $\dots, P_{t-1}, P_t, P_{t+1}, \dots$ , we seek to find a temporally consistent output  $\dots, O_{t-1}, O_t, O_{t+1}, \dots$ . Our method is agnostic to the stylization technique  $f$  applied to each frame, where  $P_t = f(I_t)$ . However, it is necessary for  $f$  to not introduce significant shape or content inconsistencies between consecutive frames, as the changes in the stylized frames should correspond to the optical flow (calculated based on the content). We initialize the consistent output for the first frame as its per-frame processed result i.e.,  $O_1 = P_1$ . To obtain the output for subsequent frames ( $O_t$  at any given instance  $t$ ) we require only a snippet of input ( $I_{t-1}, I_t, I_{t+1}$ ) and processed streams ( $P_{t-1}, P_t, P_{t+1}$ ), and the consistent output at the previous instance  $O_{t-1}$ . For enforcing consistency, we solve the following gradient-domain optimization scheme:

$$E(O_t) = \int_{\Omega} \left( \underbrace{\|\nabla O_t - \nabla P_t\|^2}_{\text{data}} + \underbrace{wc\|O_t - A_t\|^2}_{\text{smoothness}} \right) d\Omega. \quad (1)$$

where  $\Omega$  represents the image domain. The data term in this optimization enforces similarity with the per-frame processed result  $P_t$  in the gradient-domain. Thus, high-frequency details are taken from  $P_t$  and the smoothness term enforces temporal-consistency where low-frequency content is taken from the image  $A_t$ . The optimization formulation in Eqn. 1 is commonly known as *screened Poisson equation* and has been successfully employed for various image

Table 2: Constituent elements of smoothness term in Eqn. 1 for different methods. Here,  $w_s$  and  $T_d$  refers to saliency-based weights and temporally-denoised image respectively, introduced by Shekhar *et al.*

Method	Weight	Consistent Image
Ours	$w_c$	$A_t$
Bonneel <i>et al.</i> [BTS*15]	$w_p$	$\Gamma(O_{t-1})$
Shekhar <i>et al.</i> [SST*19]	$w_s$	$T_d$

editing applications [BCCZ08, BZCC10]. In the context of consistent video filtering, it was first used by Bonneel *et al.* [BTS\*15] followed by Shekhar *et al.* [SST\*19] (Tab. 2). However, our novelty is the way in which we construct our *smoothness* term which, unlike previous approaches, considers both *global* and *local* consistency aspects. Our novel smoothness term is able to better preserve the color and textures in the stylized output while providing both short-term and long-term temporal consistency.

**Local Consistency.** For enforcing temporal consistency at a local level, we use optic-flow to warp neighboring per-frame processed results to the current time instance  $t$ . This is performed by computing an adaptive combination of (1) warped previous per-frame processed image  $\Gamma(P_{t-1})$ , (2) warped next per-frame processed image  $\Gamma(P_{t+1})$ , and (3) the current per-frame processed image  $P_t$ , where  $\Gamma$  is the warping function. By including both backward and forward warping in our formulation, we are able to significantly reduce artefacts due to occlusion and flow inaccuracies. The linear combination of (1), (2), and (3) gives us a locally consistent version  $L_t$  where,

$$L_t = (1 - (wp + wn)) \cdot P_t + wp \cdot \Gamma(P_{t-1}) + wn \cdot \Gamma(P_{t+1}). \quad (2)$$

The weights  $wp$  and  $wn$  capture the inaccuracies in the warping of previous and next frames respectively and are defined as follows:

$$\begin{aligned} wp &= \exp(-\alpha\|I_t - \Gamma(I_{t-1})\|^2) \text{ and} \\ wn &= \exp(-\alpha\|I_t - \Gamma(I_{t+1})\|^2). \end{aligned} \quad (3)$$

In order to also incorporate contribution from  $P_t$ , we clamp the weights  $wp$  and  $wn$  as follows:  $\lceil wp \rceil = k_1$  and  $\lceil wn \rceil = k_2$ , where  $k_1$  and  $k_2$  are two constants. The locally consistent image sequence given by  $L_t$  has improved temporal consistency over the per-frame processed output, however, it still has visible flickering artifacts. Thus, the reduction in flickering due to warping of only one temporal neighbor is not sufficient. To further improve consistency, one can warp more neighboring frames around the current time instance  $t$ . As we increase the temporal window-size for such an adaptive combination it has a denoising effect leading to further reduction in flickering. The temporal denoising for enforcing consistency, performed by Shekhar *et al.* [SST\*19] can be considered as an specific example of the above scenario. However, for interactive stylization warping more frames to the current instance is not feasible due to time constraint. Moreover, in case of video streams we do not have frames to warp from the forward temporal direction.

**Global Consistency.** In order to overcome this limitation, existing approaches [BTS\*15, LHW\*18] adopt a global approach. For global consistency, one can consider the previous stabilized output  $O_{t-1}$  and enforce similarity with its warped version  $G_t$  where,

$$G_t = \Gamma(O_{t-1}). \quad (4)$$

To enforce only global temporal smoothness, we replace  $A_t$  with  $G_t$  in Eqn. 1. Further, in order to compensate for optic-flow inaccuracies, the smoothness term is weighted using  $wp$  (i.e.,  $wc = wp$ ) in Eqn. 1. However, considering only global consistency for flicker reduction leads to loss of stylization and local temporal variations in the final output. Moreover, in this case any warping-error (due to flow-inaccuracies) or noise (as part of stylization process)

keeps getting propagated to future frames. Due to the above factors, such an approach only gives plausible results where the gradients of the original video are similar to the gradients of the processed video. The above does not hold for the task of stylization where stylistic elements such as brush strokes, textures or stroke textons [ZGXW05], in general, can vary largely between frames even for small changes in gradient.

**Combining Global and Local Consistency.** For preserving local temporal variations (in terms of look and feel) while significantly reducing the flickering artifacts, we linearly combine globally and locally consistent images  $G_t$  and  $L_t$  respectively,

$$A_t = wp \cdot G_t + (1 - wp) \cdot L_t. \quad (5)$$

We use the adaptively combined image  $A_t$  as our reference for consistency while enforcing temporal smoothness in Eqn. 1. The  $\lceil wp \rceil$  can be increased to increase the influence of global-temporal smoothness and vice versa. Further, the influence of the smoothness term is controlled by per-pixel consistency weights  $wc$ . We would like to invoke the smoothness term only when the warping accuracy is sufficiently high. To this end, we construct a warped version of the input image similar to  $L_t$  as,

$$A^I_t = (1 - (wp + wn)) \cdot I_t + wp \cdot \Gamma(I_{t-1}) + wn \cdot \Gamma(I_{t+1}). \quad (6)$$

Only when the input image  $I_t$  is similar to  $A^I_t$ , the smoothness term is invoked. To measure this similarity, we use the weight  $wc$ ,

$$wc = \lambda \cdot \exp \left( -\alpha \cdot \left\| I_t - A^I_t \right\|^2 \right). \quad (7)$$

The parameter  $\lambda$  is used to scale up or down the weight  $wc$ .

**Consistency Control Modes.** The above adaptive combination of local and global consistency provides two different ways of consistency-control in the final output. By increasing  $\lceil wp \rceil$  we can increase the proportion of global consistency in the adaptively combined image  $A_t$  and vice versa. On the other hand the optimization parameter  $\lambda$  dictates how close the output  $O_t$  will be to the adaptively combined image  $A_t$ . Thus, the level of consistency in the final output can be controlled in two different ways: (1) by setting up the limit of parameter  $w_p$ , i.e.,  $\lceil wp \rceil$  or (2) by scaling the weight parameter  $\lambda$ . For lower values of  $\lceil wp \rceil$  (Fig. 6b), the consistency enforced is negligible and the final result resembles the per-frame processed output (Fig. 6f). However, for higher values we start observing noisy ghosting artefacts (Fig. 6e). The lower values of  $\lceil wp \rceil$  translates to using only global consistency which results in accumulation of flow inaccuracies visualized as ghosting artefacts. Similarly, for lower values of  $\lambda$  (Fig. 6g), the final result is visually similar to the per-frame processed output (Fig. 6f). However, for higher values the optimization becomes unstable resulting in noisy optimization-based artefacts. (Fig. 6j).

**Optimization Solver.** The energy terms in Eqn. 1 are smooth and convex in nature, which allows a straightforward energy minimization with respect to  $O_t$ . To this end, we employ an iterative approach thus avoiding – storage of a large matrix in memory and further estimating its inverse. Moreover, an iterative approach allows us to stop the solver once we have achieved visually plausible results. An iterative update  $O_t^{k+1}$  is obtained by employing

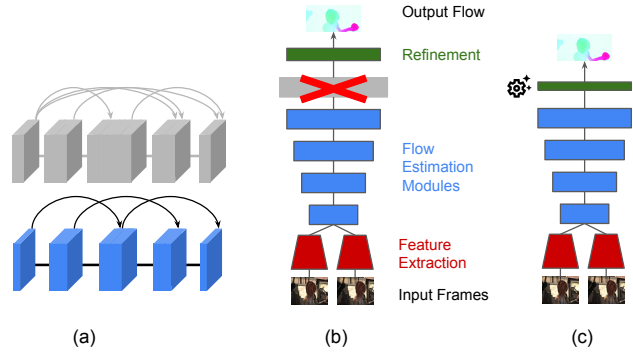


Figure 3: Modification of the PWC-Net [SYLK18] architecture for real-time performance. We apply following network compression steps: (a) Replace DenseNet connections with light ones, (b) Reduce the number of flow estimators, and (c) Replace dense connections in the refinement module with separable convolutions.

Stochastic Gradient Descent (SGD) with momentum [Qia99],

$$O_t^{k+1} = O_t^k - \eta \nabla E(O_t^k) + \kappa (O_t^k - O_t^{k-1}). \quad (8)$$

where  $\eta$  and  $\kappa$  are the step size parameters,  $\nabla E$  is the energy gradient with respect to  $O_t$ , and  $k$  is the iteration count. For most of our experiments,  $\eta = 0.15$  and  $\kappa = 0.2$  yield plausible results. We consider the trade-off between performance vs. accuracy as a stopping criteria and do not compute energy residue for this purpose. To obtain a consistent output while having interactive performance, we empirically determine 150 iterations to be sufficient. The optimization is stable for the given parameter settings and early stopping is only employed for computational gain.

An integral aspect common to both our *local* and *global* consistency is the warping function  $\Gamma$ . Apart from the number of solver iterations, for interactive performance the above warping should also happen at a fast rate – which in turn necessitates fast optic-flow estimation.

### 3.2. Lite Optic-Flow Network

We aim to obtain a flow network capable of running at high-speed on consumer hardware with reasonable accuracy. To this end, we start by selecting an existing CNN-based optical flow estimation technique, based on accuracy vs. run-time analysis. After the selection of a base network, we perform further optimization steps to increase the performance as outlined in Fig. 3.

**Base Network Selection for Compression.** In Fig. 4, we compare several well-known optical methods to find a base network candidate that best matches our runtime/accuracy requirements. We employ the following models for this: FlowNet 2.0 [IMS\*17], SpyNet [RB17], LiteFlowNet2 [HTL20], PWCNet [SYLK18], ARFlow [LZH\*20], VCN [YR19], RAFT [TD20] and finally GMA [JCL\*21] (state-of-the-art in terms of EPE-based accuracy). Our experiments are carried out on a Nvidia RTX 2070 GPU, which we deem to be a good representative of a current mid-to

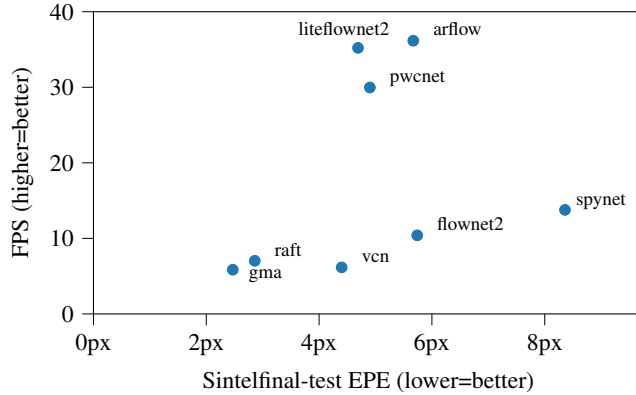


Figure 4: Accuracy vs. run-time performance of existing methods measured on Sintel Final (Test set) [BWSB12]. The Endpoint Error (EPE) metric measures Euclidean distance (in pixels) between ground-truth and predicted optical flow vectors.

higher-end consumer GPU. Under a constraint of interactive performance on consumer hardware, LiteFlowNet2 [HTL20] and PWC-Net [SYLK18] offer the best trade-off between run-time performance and accuracy (Fig. 4). LiteFlowNet2 [HTL20] is already an optimized version of FlowNet 2.0 [IMS\*17], in comparison PWC-Net [SYLK18] has more potential for optimization/compression. Moreover, recently it has been shown that PWC-Net can achieve similar accuracy to RAFT when trained on a large-scale synthetic dataset [SVH\*21] and that PWC-Net achieves favourable trade-offs vs. other state-of-the-art methods when selecting for runtime performance or higher image resolutions [SHR\*22]. Hence, we select PWC-Net for further compression.

**Optimized Network Architecture.** We start with the base architecture of PWC-Net. As the first compression step we reduce the computationally expensive DenseNet [HLvdMW17] connections in the flow estimators to retain connections only in the last two layers ("light" in Fig. 5b). Similar to LiteFlowNet2 [HTL20], we remove the fifth flow estimator – operating on the highest resolution – as it heavily trades off run-time for only marginal increase in accuracy (compare "4light" vs "5light" in Fig. 5b). We replace the standard convolutions in the refinement by depthwise separable convolutions [HZA\*17] ("sepref" in Fig. 5b). Moreover, we also explore reducing the number of channels [HZA\*17], but find that reducing channels results in a worse trade-off as compared to other optimizations.

**Training.** For training, we follow the original PWC-Net [SYLK18] schedule. However, we find that weighting the multi-scale losses equally, instead of exponentially [SYLK18, HTL18, HTL20, YR19], improves accuracy. For our experiments on the desktop system, we use PyTorch [PGM\*19] and take inspiration from the implementation by Niklaus [Nik18]. Similar to PWC-Net [SYLK18], we train our mobile architecture on the training dataset schedule FlyingChairs [FDI\*15] → FlyingThings3D [MIH\*16] → Sintel [BWSB12]. In the supplementary material, we provide training settings for each stage in detail. We

Table 3: Runtime performance in milliseconds per frame. We measure the total processing time (without disk IO) and the individual stages for a mid-tier GPU (Nvidia GTX 1080Ti) and a higher-end GPU (Nvidia RTX 3090), results are averaged over 100 runs.

Task ↓ Res. / GPU	Optical flow		Stabilization		Total	
	1080Ti	3090	1080Ti	3090	1080Ti	3090
1920 × 1080 px	66.8	40.0	184.1	42.7	250.8	82.7
1280 × 720 px	31.3	19.7	86.5	21.1	117.8	40.8
640 × 480 px	12.6	6.2	20.6	6.3	33.2	12.5

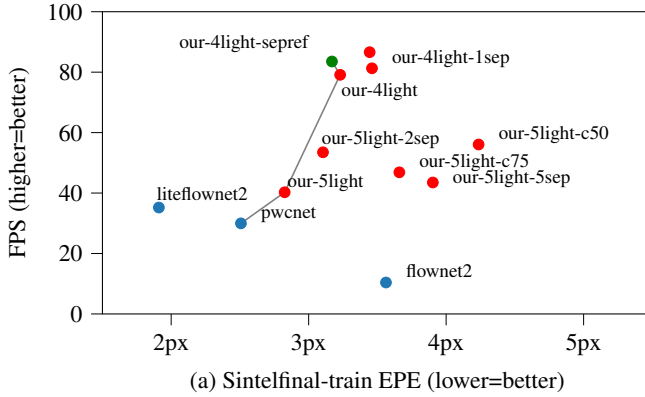
employ a multi-scale loss [SYLK18] applied to each flow estimator and optimize using the AdamW optimizer [LH19] with  $\beta_1 = 0.09$ ,  $\beta_2 = 0.99$ , and  $l_2$  weight regularization with trade-off  $\gamma = 0.0004$ . Furthermore, extensive dataset augmentation is applied to prevent model overfitting. We refer to the supplementary material for more details.

**Our Final Model.** We analyze various optimization options and chose “our-4light-sepref” as our final model for desktop systems as it provides the best trade-off between accuracy vs. run-time. As depicted in Fig. 5a, our method improves run-time performance of PWC-Net from 30 FPS to 85 FPS – a speed-up of factor 2.8. For Sintel training data the accuracy drops by  $\approx 0.5$ px in EPE terms, however for test data the drop in accuracy is significant where the final EPE is 7.43. Nevertheless, the accuracy is sufficient enough for enforcing warping-based consistency. To validate our design decisions, we conduct an extensive ablation study in which we vary the architectural and training choices – please see the supplementary for details. Furthermore, we tune our architecture for optical flow calculation on mobile devices using channel pruning and quantization, which we also detail in the supplementary material. Here, we improve run-time performance from 2.8 FPS to 24 FPS (iPad Pro 2020), and 1.5 FPS to 13 FPS (iPad Air) – an improvement of factor 8. Next to showing the general applicability of optical flow CNNs on mobile devices, this demonstrates that real-time on-device stabilization of videos using our presented approach will become feasible with a further moderate increase in mobile GPU computing power. A fast optic-flow based warping enables our framework to interactively control the degree of consistency and generate visually plausible results.

## 4. Experimental Results

### 4.1. Implementation Details

All our experiments were performed on a consumer PC with an AMD Ryzen 1920X 12-Core CPU, 48 GB of RAM, and a Nvidia GTX 1080Ti and RTX 3090 graphics cards with VRAMs of 11 GB and 24 GB respectively. We implement a real-time video-consistency framework in C++, using ONNXRuntime for cross-platform acceleration of our lite optical-flow network and implement the stabilization code using Nvidia CUDA (v11.4). In Tab. 3, we measure the runtime performance of our system. We find that an incoming stream of frames can be stabilized at real-time performance for VGA resolution even on low- and mid-tier GPUs and higher-tier GPUs (such as a RTX 3090) can stabilize HD at common video frame rates (approx. 24 FPS) and full-HD resolutions at



Modifier	Description	Default
-Nlight	$N$ light [LZH*20] flow estimators.	5 dense [SYLK18]
-Msep	last $M$ flow estimators use depthwise separable convolutions [HZA*17].	standard convs.
-sepref	refinement uses depthwise separable convolutions [HZA*17].	standard convs.
-cP	use $P\%$ of channels.	100%

(b) Legend of our CNN variants.

Figure 5: Accuracy vs. run-time performance of our CNN variants on desktop, measured on Sintel Final (Train) [BWSB12]. Optimization steps that lead to significant improvement in run-time are connected by a line. Our architectural modifications to PWC-Net [SYLK18] are detailed on the right, e.g., our-4light-sepref denotes a 4 light flow estimators and refinement using depthwise separable convolutions.

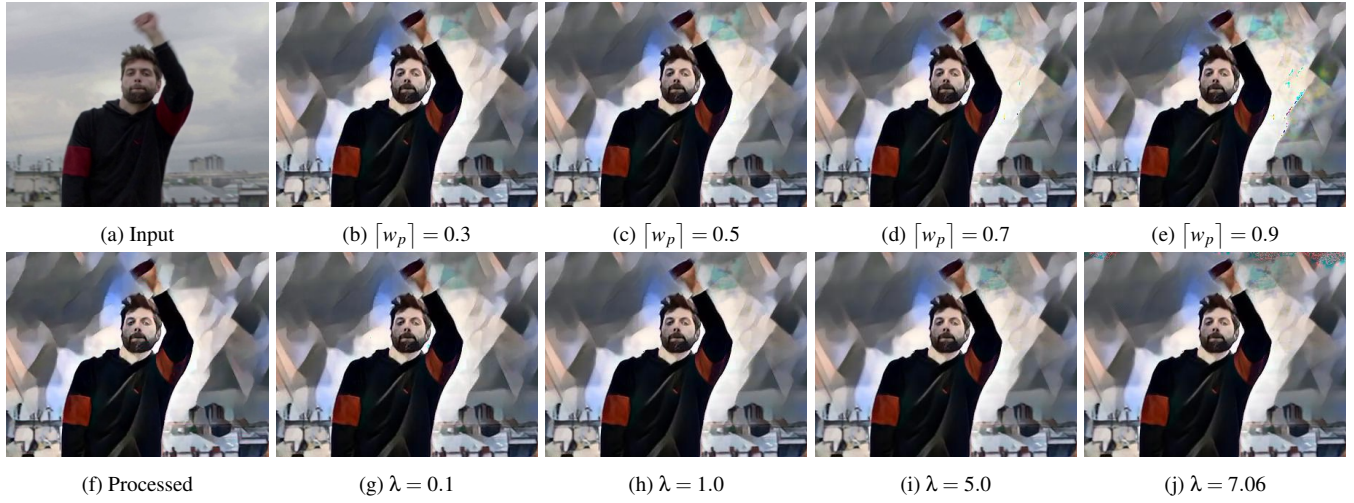


Figure 6: The level of consistency in the final output can be controlled via parameters  $[w_p]$  and  $\lambda$ . Here we show how the final result vary by increasing these, for lower values the consistency is negligible and the results (Fig. 6b and Fig. 6g) visually look similar to the per-frame processed output (Fig. 6b). For higher values we start observing artefacts due to ghosting and/or optimization (Fig. 6e and Fig. 6j).

interactive frame rates ( $> 10$  FPS) for different parameter settings (Tab. 3).

#### 4.2. Parameter Settings

Initially, we tune the parameters of our consistency framework towards achieving a low warping error (Tab. 5). We refer to this setting as *Ours-objective* with the following parameter values  $k_1 = k_2 = 0.3$ ,  $\alpha = 10 \times 10^3$ , and  $\lambda = 0.7$ . However, we observed that even though the warping error indicated a good temporal stability, subjectively flickering and artefacts were noticeable. Unlike existing approaches, our framework allows for interactive parameter adjustment. Thus, a parameter set that subjectively produces well-stabilized results on a broad range of tasks and videos was obtained experimentally. As our final version, we use the values of  $k_1 = 0.3$ ,  $k_2 = 0.5$ ,  $\alpha = 6.5 \times 10^3$ , and  $\lambda = 2.0$  to generate all the images in

the paper and the videos provided in the supplementary. We further compare *Ours-objective* settings with our final version as part of our user study to validate our parameter choices. The consistent outputs obtained using the above parameter settings are compared against state of the art approaches thereby showcasing its efficacy.

#### 4.3. Consistent Outputs

We use videos from DAVIS [PPTM\*16] dataset and other open source videos (taken from [Vid] and [Pex]) for comparison. For per-frame stylization, we employ the following stylization techniques: Fast NST [JAFF16], WCT [LFY\*17], and CycleGAN [ZPIE17]. The results for the method of Lai *et al.* and Bonneel *et al.* on videos taken from DAVIS [PPTM\*16] and Videvo ([Vid]) are borrowed from the *results* dataset provided by Lai *et al.*. For other videos we employ the source code provided by the authors to generate

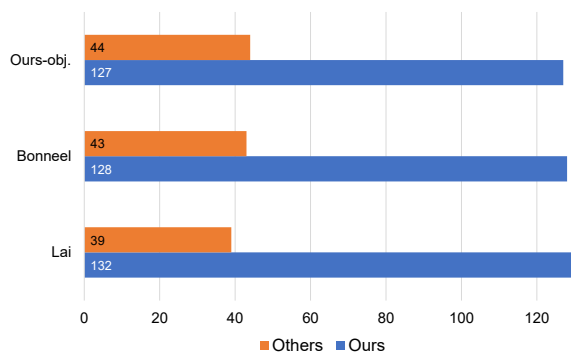


Figure 7: Statistics of the user study results on removal of temporal flickering from per-frame stylized videos. For 19 participants and 9 different videos we compare our method against Bonneel *et al.*, Lai *et al.*, and *Ours-objective* through a total of 171 randomized A/B tests.

the results. We compare our consistent outputs with that of Bonneel *et al.* [BTS\*15] and Lai *et al.* [LHW\*18] in Fig. 8. Among the three competing methods Bonneel *et al.* is the least effective in preserving the underlying style for the final output (compare second column with the fourth one in Fig. 8). Hyper-parameter tuning in the above method (with only global consistency) can provide a certain degree of consistency-control. However, by employing both global and local consistency we achieve finer consistency-control while being similar to the per-frame-processed result. For the method of Lai *et al.*, we observe some color bleeding or darkening in the output frames (compare second column with the third one in Fig. 8). In comparison we are able to preserve the style, color and textures, while being consistent (Fig. 7).

#### 4.4. Optic Flow Results

We visualize optical flow on frames from the Sintel [BWSB12] dataset in Fig. 9 and compare to state-of-the-art methods. All depicted methods have been fine-tuned on Sintel. We find that our optimized method has more blurry motion boundaries and misses to estimate certain details accurately (e.g., the hand in the first row, however, PWCNet also fails at this), but still captures overall motion direction of objects correctly with a smooth flow field. Fig. 10 shows results for real-world videos on the DAVIS dataset [PTPC\*17] (no ground-truth flow available). We find that some real-world image phenomena, such as complex/ambiguous occlusions (e.g., bus behind tree) are not well-handled by state-of-the-art methods like RAFT [TD20] or PWC-Net [SYLK18], and thus results are degraded for our optimized method as well. Besides the stronger blurred motion boundaries, we find that our network generally performs well and is also robust for real-world videos.

## 5. Evaluation

### 5.1. Quantitative

Following Lai *et al.* [LHW\*18], we measure the similarity between per-frame processed output and stabilized results, and the temporal warping error between consecutive stabilized frames.

For the former, we report the similarity in form of the SSIM metric in Tab. 4. We achieve significantly higher similarity scores than the methods of Bonneel *et al.* [BTS\*15] and Lai *et al.* [LHW\*18]. Following [BTS\*15] and [LHW\*18], we also measure the temporal warping error between a frame  $V_t$  and the warped consecutive frame  $\hat{V}_{t+1}$ , defined as:

$$E_{\text{warp}}(V_t, V_{t+1}) = \frac{1}{\sum_{i=1}^N M_t^{(i)}} \sum_{i=1}^N M_t^{(i)} \left\| V_t^{(i)} - \hat{V}_{t+1}^{(i)} \right\|_1, \quad (9)$$

where  $M_t \in \{0, 1\}$  is a non-occlusion mask [LHW\*18, RDB18], indicating non-occluded regions. The warped frame  $\hat{V}_{t+1}$  is obtained by calculating the optical flow (using GMA [JCL\*21]) between frames  $V_t, V_{t+1}$ , and applying a backwards warping to frame  $V_{t+1}$ . We compute  $E_{\text{warp}}$  for every frame of a video and then average to obtain the warping error of a video  $E_{\text{warp}}(V)$ . In Tab. 5 we report the average warping error per dataset (see the supplementary for a per-task breakdown). We find that the warping error is slightly higher than that of Bonneel *et al.* [BTS\*15] and Lai *et al.* [LHW\*18]. However, as Lai *et al.* [LHW\*18] notes, results with high temporal stability (expressed by a low warping error) can also be achieved via temporally smoothing the video, which can be seen in various results of Bonneel *et al.* [BTS\*15]. Our qualitative results in form of a user study Sec. 5.2 further substantiate the divide between warping error (as a stability metric) and perceived stability.

### 5.2. Qualitative

For qualitative evaluation we perform a subjective user study where we ask participants to compare the temporally-consistent result obtained using our method with that of Lai *et al.*, Bonneel *et al.*, and *Ours-objective* – a different parameter setting of ours. We use 9 different videos for this purpose: 3 from DAVIS [PPTM\*16], 3 from Videvo [Vid], and 3 from Pexels [Pex] datasets respectively. For each of the above video we stylize them using either the Fast NST [JAFF16] (in the styles of *udnie*, *rain-princess*, and *mosaic*) or WCT [LFY\*17] (in the styles of *wave* and *antimono*) or CycleGAN (in the styles of *photo2vangogh* and *photo2ukiyo*e). For each sample, we show the input video and its per-frame stylized version on the top row of user-study interface for inference. In the bottom row we show two different version of the temporally stabilized output where one of them is ours. We ask the participants to select the output which best preserves: (i) temporally consistency and (ii) similarity with the per-frame processed video. For 9 videos and 3 other competing methods each user sees a total of 27 blind A/B tests which are shown in a randomized order to each participant. In total, 19 persons (3 female and 16 male) within the ages of 22 to 43 years participated in the study. Fig. 7 shows that our method surpasses all others by a large margin. It was interesting to observe that for certain cases the method of Bonneel *et al.* which degrades the processed style significantly was still preferred by users over others due to its high consistency quality.

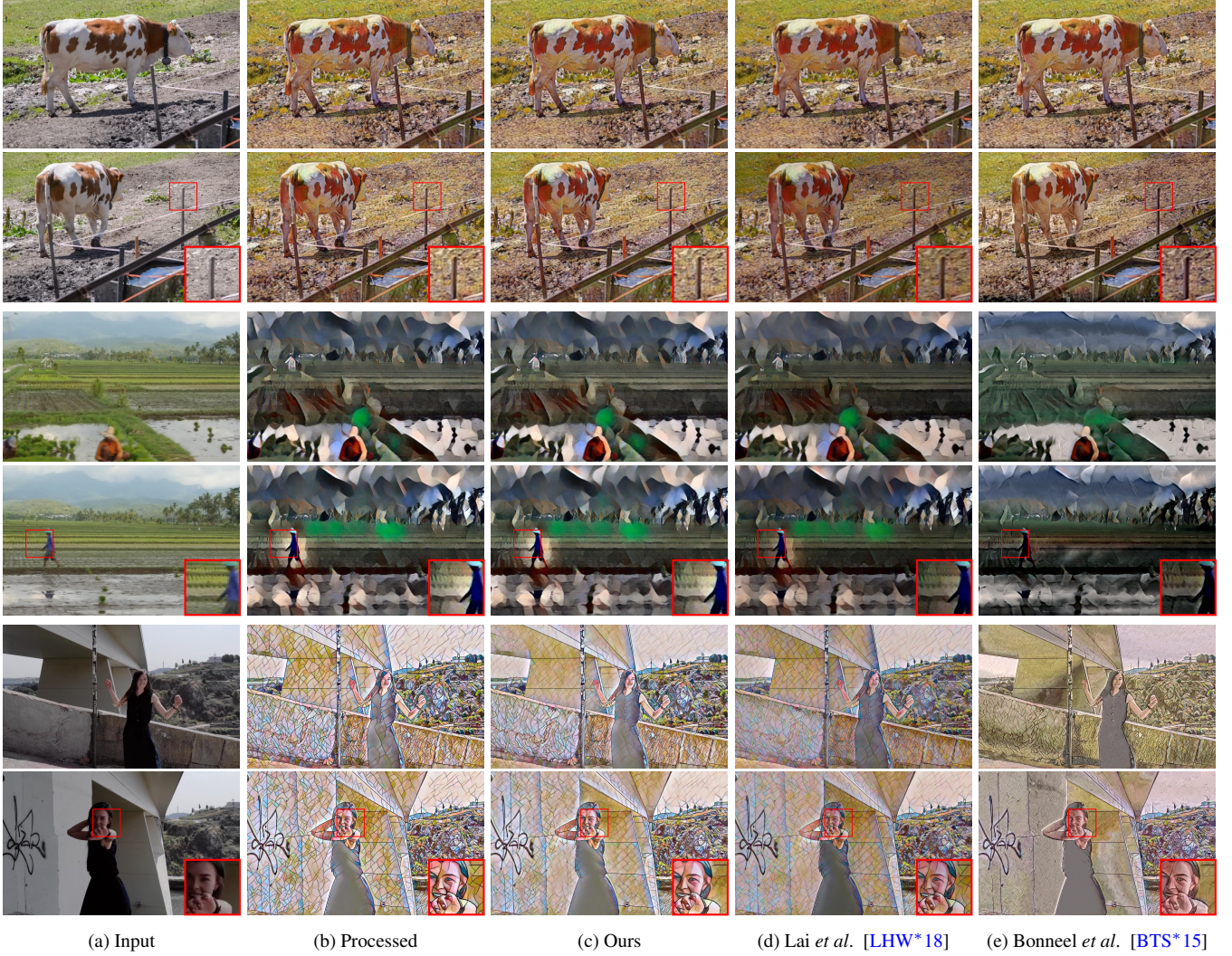


Figure 8: Comparing our results with Lai *et al.* [LHW\*18] and Bonneel *et al.* [BTS\*15] for three different video sequences: *Cow* (top two rows), *Farming* (mid two rows), and *Woman* (last two rows). Note how the consistent output for Lai *et al.* and Bonneel *et al.* look different from the corresponding per-frame processed results.

### 5.3. Using other Optical Flows

We also tested other optical flow methods within our pipeline which were either faster [KTDVG16] or more accurate [TD20]. For the fast optical method by Kroeger *et al.* [KTDVG16](DIS) the final output is less consistent than ours in both objective and subjective metrics. Using DIS for our stabilization, the average warp-error over DAVIS is 0.05 (vs. 0.046 ours) and perceptual-similarity with the per-frame processed result is 0.9 in SSIM terms (vs. 0.923 ours). Visually, DIS-stabilized results show significantly more flickering, validating our design choice for the optical-flow. A much more accurate optic flow is given by the method of Teed *et al.* [TD20] (RAFT) at the cost of slow computation. The stabilized results obtained using RAFT look visually indistinguishable to the one obtained using our flow; the average warp-error over DAVIS is 0.045, the perceptual-similarity is 0.923.

## 6. Discussion

Our approach takes a video pair as an input: (i) the original and (ii) its per-frame stylized version. We assume that the stylization is based on the input image-gradients and appears as variations in the form of colors and/or textures. Thereby, we employ the original video as a guide for enforcing consistency. However, for text-guided generative arts such as recent diffusion model-based approaches [RDN\*22, RBL\*22] the stylized frames are often only weakly correlated with the original input, we cannot handle such cases.

For the evaluation we mainly use CNN-based stylization techniques. However our approach can also handle classical stylization approaches [KCWI13], we show few such examples in the supplementary. Our local-consistency component comprising of convex combination of temporal neighbors can be seen as crude form of

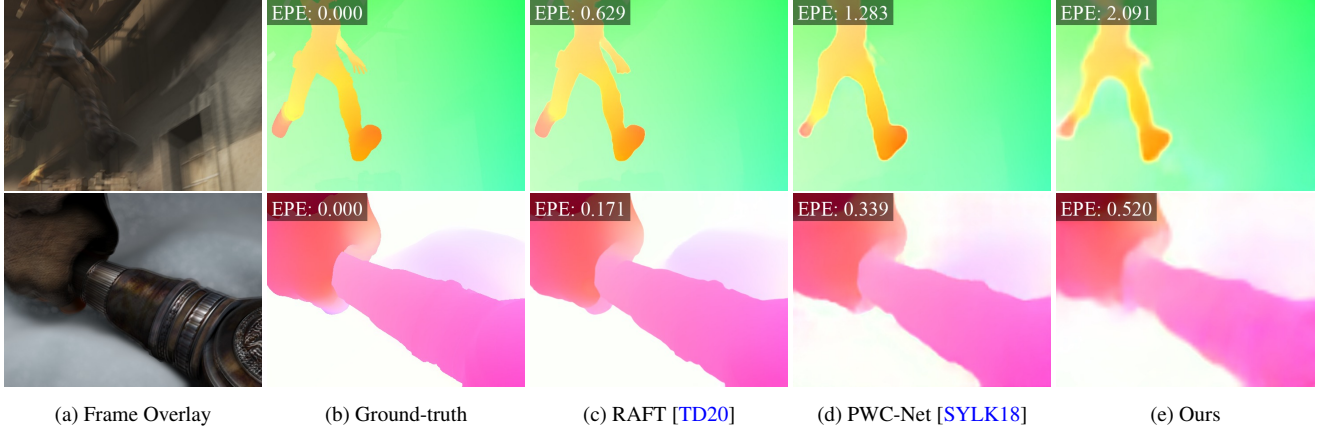


Figure 9: Optical flow estimated using the synthetic Sintel dataset [BWSB12].

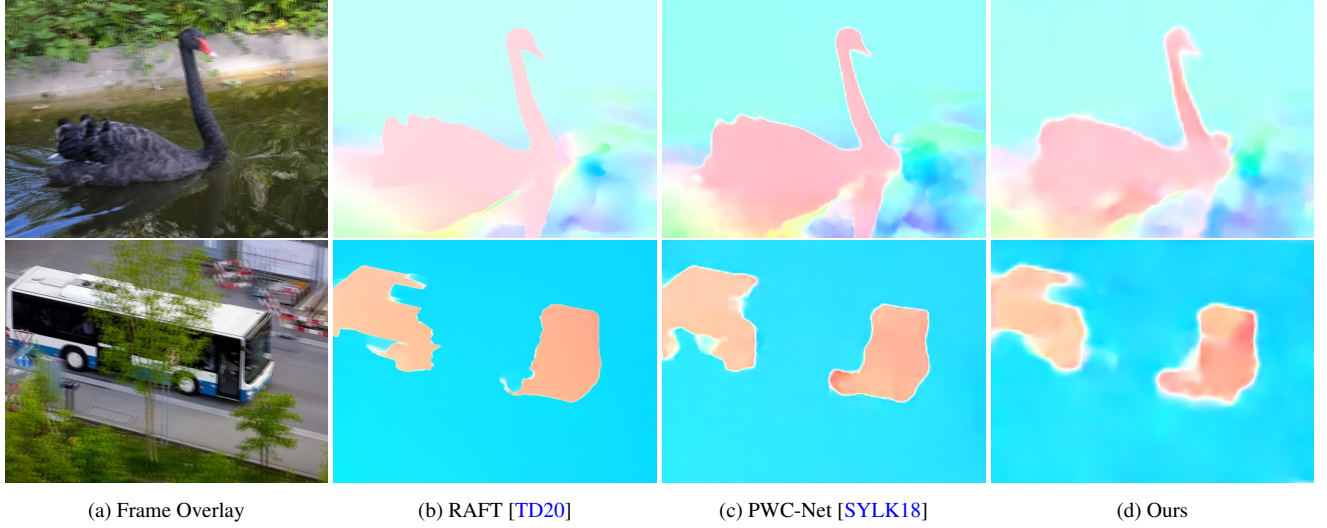
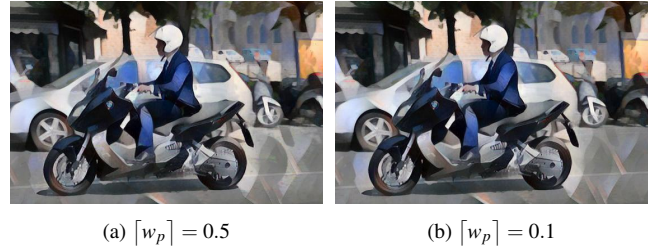


Figure 10: Optical flow estimated for the real-world dataset DAVIS [PTPC\*17].

local temporal denoising. Previously it has been shown that temporal denoising is effective in enforcing consistency [SST\*19]. We conjecture that efficient temporal-denoising combined with flow-based warping can further improve temporal stabilization not only for stylization but also for other tasks.

We start with the assumption that temporal flickering is not completely undesirable for the task of stylization and thus we provide interactive consistency control. However, during the subjective user study we observed that participants had different tolerance levels for flickering in the foreground as compared to that in the background. As part of future work, one can use depth-based or saliency-based masks to vary the consistency control parameters spatially for a more visually pleasing result.

**Limitation:** Our approach tends to have ghosting artifacts for fast moving objects where the object motion between consecutive frames is large (Fig. 11). The above can be reduced by reducing the value of  $\lceil w_p \rceil$ , however such a reduction also reduces consistency in the final output. We argue that since we provide interactive control of parameters the above trade off between artifacts vs. consistency will not hinder its usability significantly.

Figure 11: The ghosting artifacts on the rear wheel of the scooter is significant in the final output for  $\lceil w_p \rceil = 0.5$ , however it reduces significantly for  $\lceil w_p \rceil = 0.1$ .

tency in the final output. We argue that since we provide interactive control of parameters the above trade off between artifacts vs. consistency will not hinder its usability significantly.

Table 4: Quantitative evaluation on perceptual distance using SSIM (higher = more similar to per-frame processed result).

Task	DAVIS			VIDEVO		
	[BTS*15]	[LHW*18]	Ours	[BTS*15]	[LHW*18]	Ours
CycleGAN/photo2ukiyo [ZPIE17]	0.693	0.781	<b>0.978</b>	0.626	0.743	<b>0.980</b>
CycleGAN/photo2vangogh [ZPIE17]	0.707	0.792	<b>0.961</b>	0.679	0.789	<b>0.965</b>
fast-neural-style/rain-princess [JAFF16]	0.553	0.799	<b>0.921</b>	0.491	0.796	<b>0.920</b>
fast-neural-style/udnie [JAFF16]	0.597	0.785	<b>0.956</b>	0.579	0.747	<b>0.959</b>
WCT/antimonocromatismo [LFY*17]	0.389	0.811	<b>0.915</b>	0.388	0.761	<b>0.914</b>
WCT/asheville [LFY*17]	0.329	0.801	<b>0.904</b>	0.348	0.771	<b>0.901</b>
WCT/candy [LFY*17]	0.289	0.763	<b>0.882</b>	0.310	0.738	<b>0.885</b>
WCT/feathers [LFY*17]	0.418	0.863	<b>0.891</b>	0.415	0.848	<b>0.888</b>
WCT/sketch [LFY*17]	0.370	0.845	<b>0.923</b>	0.370	0.833	<b>0.922</b>
WCT/wave [LFY*17]	0.358	0.700	<b>0.902</b>	0.352	0.637	<b>0.899</b>
Average	0.470	0.794	<b>0.923</b>	0.456	0.766	<b>0.923</b>

Table 5: Flow warping error average over tasks shown in Tab. 4. A per-task breakdown is shown in the supplementary. Note that the slightly higher warping error (lower is better) of our method is subjectively not noticeable as we show in a user study.

Dataset	$V_p$	[BTS*15]	[LHW*18]	Ours
DAVIS	0.056	0.034	0.040	0.046
VIDEVO	0.051	0.036	0.036	0.042

## 7. Conclusions

We propose an approach that makes per-frame stylized videos temporally coherent irrespective of the underlying stylization applied on individual frames. At this, we introduce a novel temporal consistency prior which combines both local and global consistency aspects. We maintain similarity with the per-frame processed result by minimizing the difference in the gradient-domain. Unlike previous approaches we provide interactive consistency control by computing optic-flow on the incoming video stream with only sufficient accuracy but at high speed. Fast optic-flow inference is achieved by developing a lightweight flow network architecture based on PWC-Net. The entire optimization solving is GPU-based and runs at real-time frame-rates for HD resolution. We showcase that our temporally consistent output is preferred over the output of competing methods by conducting a user study. As part of future work we would like to employ learning-based temporal denoising to further improve quality of results. Moreover, we would like to explore the usage of depth-based and saliency-based masks to spatially vary consistency parameters according to perceptual principles. We hope that our design paradigm of interactive consistency control will potentially make per-frame video stylization more user friendly.

## References

[BCCZ08] BHAT P., CURLESS B., COHEN M., ZITNICK C. L.: Fourier analysis of the 2d screened poisson equation for gradient domain problems. In *Computer Vision – ECCV 2008* (2008), Springer Berlin Heidelberg, pp. 114–128. [doi:10.1007/978-3-540-88688-4\\_9](https://doi.org/10.1007/978-3-540-88688-4_9) 4

[BCK\*13] BÉNARD P., COLE F., KASS M., MORDATCH I., HEGARTY J., SENN M. S., FLEISCHER K., PESARE D., BREEDEN K.: Stylizing submitted to 200x.

[BLV\*10] BÉNARD P., LAGAE A., VANGORP P., LEFEBVRE S., DRETTAKIS G., THOLLLOT J.: A dynamic noise primitive for coherent stylization. *Computer Graphics Forum* 29, 4 (2010), 1497–1506. [doi:https://doi.org/10.1111/j.1467-8659.2010.01747.x](https://doi.org/10.1111/j.1467-8659.2010.01747.x) 1

[BNTS07] BOUSSEAU A., NEYRET F., THOLLLOT J., SALESIN D.: Video watercolorization using bidirectional texture advection. *ACM Trans. Graph.* 26, 3 (jul 2007), 104–es. [doi:10.1145/1276377.1276507](https://doi.org/10.1145/1276377.1276507) 1, 3

[BSFG09] BARNES C., SHECHTMAN E., FINKELSTEIN A., GOLDMAN D. B.: Patchmatch: A randomized correspondence algorithm for structural image editing. *ACM Trans. Graph.* 28, 3 (jul 2009). [doi:10.1145/1531326.1531330](https://doi.org/10.1145/1531326.1531330) 3

[BTC13] BÉNARD P., THOLLLOT J., COLLOMOSSE J.: *Temporally Coherent Video Stylization*. 2013, pp. 257–284. [doi:10.1007/978-1-4471-4519-6\\_13](https://doi.org/10.1007/978-1-4471-4519-6_13) 1, 3

[BTS\*15] BONNEEL N., TOMPKIN J., SUNKAVALLI K., SUN D., PARIS S., PFISTER H.: Blind video temporal consistency. *ACM Trans. Graph.* 34, 6 (oct 2015). [doi:10.1145/2816795.2818107](https://doi.org/10.1145/2816795.2818107) 1, 2, 4, 8, 9, 11

[BWSB12] BUTLER D. J., WULFF J., STANLEY G. B., BLACK M. J.: A naturalistic open source movie for optical flow evaluation. In *European Conference on Computer Vision (ECCV)* (2012), pp. 611–625. [doi:10.1007/978-3-642-33783-3\\_44](https://doi.org/10.1007/978-3-642-33783-3_44) 6, 7, 8, 10

[BZCC10] BHAT P., ZITNICK C. L., COHEN M., CURLESS B.: Gradientshop: A gradient-domain optimization framework for image and video filtering. *ACM Trans. Graph.* 29, 2 (2010). [doi:10.1145/1731047.1731048](https://doi.org/10.1145/1731047.1731048) 4

[CLY\*17] CHEN D., LIAO J., YUAN L., YU N., HUA G.: Coherent online video style transfer. In *2017 IEEE International Conference on Computer Vision (ICCV)* (2017), pp. 1114–1123. [doi:10.1109/ICCV.2017.126](https://doi.org/10.1109/ICCV.2017.126) 3, 4

[DBZY15] DONG X., BONEV B., ZHU Y., YUILLE A. L.: Region-based temporally consistent video post-processing. In *2015 IEEE Conference on Computer Vision and Pattern Recognition (CVPR)* (2015), pp. 714–722. [doi:10.1109/CVPR.2015.7298671](https://doi.org/10.1109/CVPR.2015.7298671) 2

[DTD\*21] DENG Y., TANG F., DONG W., HUANG H., MA C., XU C.: Arbitrary video style transfer via multi-channel correlation. *Proceedings of the AAAI Conference on Artificial Intelligence* 35, 2 (May 2021), 1210–1217. URL: <https://ojs.aaai.org/index.php/AAAI/article/view/16208> 3

[FDI\*15] FISCHER P., DOSOVITSKIY A., ILG E., HÄUSSER P., HAZIRBAS C., GOLKOV V., VAN DER SMAGT P., CREMERS D., BROX

T.: Flownet: Learning optical flow with convolutional networks. In *International Conference on Computer Vision (ICCV)* (2015), p. 2758–2766. [doi:10.1109/ICCV.2015.316](https://doi.org/10.1109/ICCV.2015.316). 6

[FKL\*21] FUTSCHIK D., KUČERA M., LUKÁČ M., WANG Z., SHECHTMAN E., SÝKORA D.: Stalp: Style transfer with auxiliary limited pairing. *Computer Graphics Forum* 40, 2 (2021), 563–573. [doi:https://doi.org/10.1111/cgf.142655](https://doi.org/10.1111/cgf.142655). 1, 4

[FLJ\*14] FIŠER J., LUKÁČ M., JAMRIŠKA O., ČADÍK M., GINGOLD Y., ASENTE P., SÝKORA D.: Color me noisy: Example-based rendering of hand-colored animations with temporal noise control. In *Proceedings of the 25th Eurographics Symposium on Rendering* (2014), EGSR ’14, Eurographics Association, p. 1–10. 2

[GEB16] GATYS L. A., ECKER A. S., BETHGE M.: Image style transfer using convolutional neural networks. In *2016 IEEE Conference on Computer Vision and Pattern Recognition (CVPR)* (2016), pp. 2414–2423. [doi:10.1109/CVPR.2016.265](https://doi.org/10.1109/CVPR.2016.265). 3

[GJAF17] GUPTA A., JOHNSON J., ALAHI A., FEI-FEI L.: Characterizing and improving stability in neural style transfer. In *IEEE International Conference on Computer Vision, ICCV 2017, Venice, Italy, October 22–29, 2017* (2017), pp. 4087–4096. [doi:10.1109/ICCV.2017.438](https://doi.org/10.1109/ICCV.2017.438). 3, 4

[Hae90] HAEBERLI P.: Paint by numbers: Abstract image representations. In *Proceedings of the 17th Annual Conference on Computer Graphics and Interactive Techniques* (1990), SIGGRAPH ’90, Association for Computing Machinery, p. 207–214. [doi:10.1145/97879.97902](https://doi.org/10.1145/97879.97902). 1

[HLvdMW17] HUANG G., LIU Z., VAN DER MAATEN L., WEINBERGER K. Q.: Densely connected convolutional networks. In *Computer Vision and Pattern Recognition (CVPR)* (2017), pp. 2261–2269. [doi:10.1109/CVPR.2017.243](https://doi.org/10.1109/CVPR.2017.243). 6

[HTL18] HUI T.-W., TANG X., LOY C. C.: Liteflownet: A lightweight convolutional neural network for optical flow estimation. In *Computer Vision and Pattern Recognition (CVPR)* (2018), pp. 8981–8989. [doi:10.1109/CVPR.2018.00936](https://doi.org/10.1109/CVPR.2018.00936). 3, 6

[HTL20] HUI T. W., TANG X., LOY C. C.: A lightweight optical flow cnn - revisiting data fidelity and regularization. In *Transactions on Pattern Analysis and Machine Intelligence (TPAMI)* (2020). [doi:10.1109/TPAMI.2020.2976928](https://doi.org/10.1109/TPAMI.2020.2976928). 3, 5, 6

[HWL\*17] HUANG H., WANG H., LUO W., MA L., JIANG W., ZHU X., LI Z., LIU W.: Real-time neural style transfer for videos. In *2017 IEEE Conference on Computer Vision and Pattern Recognition (CVPR)* (2017), pp. 7044–7052. [doi:10.1109/CVPR.2017.745](https://doi.org/10.1109/CVPR.2017.745). 3, 4

[HZC\*17] HOWARD A. G., ZHU M., CHEN B., KALENICHENKO D., WANG W., WEYAND T., ANDRETTI M., ADAM H.: Mobilenets: Efficient convolutional neural networks for mobile vision applications. In *CoRR* (2017). [arXiv:1704.04861](https://arxiv.org/abs/1704.04861). 6, 7

[IMS\*17] ILG E., MAYER N., SAIKIA T., KEUPER M., DOSOVITSKIY A., BROX T.: Flownet 2.0: Evolution of optical flow estimation with deep networks. In *Computer Vision and Pattern Recognition (CVPR)* (2017), pp. 1647–1655. [doi:10.1109/CVPR.2017.179](https://doi.org/10.1109/CVPR.2017.179). 3, 5, 6

[JAFF16] JOHNSON J., ALAHI A., FEI-FEI L.: Perceptual losses for real-time style transfer and super-resolution. In *Computer Vision – ECCV 2016* (2016), Leibe B., Matas J., Sebe N., Welling M., (Eds.), pp. 694–711. [doi:10.1007/978-3-319-46475-6\\_43](https://doi.org/10.1007/978-3-319-46475-6_43). 7, 8, 11

[JCL\*21] JIANG S., CAMPBELL D., LU Y., LI H., HARTLEY R.: Learning to estimate hidden motions with global motion aggregation. In *Proceedings of the IEEE/CVF International Conference on Computer Vision* (2021), pp. 9772–9781. 2, 3, 5, 8

[JST\*19] JAMRIŠKA O., SOCHOROVÁ V., TEXLER O., LUKÁČ M., FIŠER J., LU J., SHECHTMAN E., SÝKORA D.: Stylizing video by example. *ACM Trans. Graph.* 38, 4 (jul 2019). [doi:10.1145/3306346.3323006](https://doi.org/10.1145/3306346.3323006). 1, 4

[JYF\*20] JING Y., YANG Y., FENG Z., YE J., YU Y., SONG M.: Neural style transfer: A review. *IEEE Transactions on Visualization and Computer Graphics* 26, 11 (2020), 3365–3385. [doi:10.1109/TVCG.2019.2921336](https://doi.org/10.1109/TVCG.2019.2921336). 1

[KCWI13] KYPRIANIDIS J. E., COLLOMOSSE J., WANG T., ISENBERG T.: State of the “art”: A taxonomy of artistic stylization techniques for images and video. *IEEE Transactions on Visualization and Computer Graphics* 19, 5 (2013), 866–885. [doi:10.1109/TVCG.2012.160](https://doi.org/10.1109/TVCG.2012.160). 1, 9

[KP11] KASS M., PESARE D.: Coherent noise for non-photorealistic rendering. *ACM Trans. Graph.* 30, 4 (jul 2011). [doi:10.1145/2010324.1964925](https://doi.org/10.1145/2010324.1964925). 1

[KTDVG16] KROEGER T., TIMOFTE R., DAI D., VAN GOOL L.: Fast optical flow using dense inverse search. In *Computer Vision – ECCV 2016* (2016), Leibe B., Matas J., Sebe N., Welling M., (Eds.), pp. 471–488. 9

[LFY\*17] LI Y., FANG C., YANG J., WANG Z., LU X., YANG M.-H.: Universal style transfer via feature transforms. In *Proceedings of the 31st International Conference on Neural Information Processing Systems* (2017), NIPS’17, p. 385–395. URL: <https://dl.acm.org/doi/10.5555/3294771.3294808>. 7, 8, 11

[LH19] LOSHCILIOV I., HUTTER F.: Fixing weight decay regularization in adam. In *International Conference on Learning Representations (ICLR)* (2019). URL: <https://openreview.net/forum?id=rk6qdGgCZ>. 6

[LHW\*18] LAI W.-S., HUANG J.-B., WANG O., SHECHTMAN E., YUMER E., YANG M.-H.: Learning blind video temporal consistency. In *Computer Vision – ECCV 2018* (2018), Ferrari V., Hebert M., Sminchisescu C., Weiss Y., (Eds.), pp. 179–195. 1, 2, 3, 4, 8, 9, 11

[Lit97] LITWINOWICZ P.: Processing images and video for an impressionist effect. In *Proceedings of the 24th Annual Conference on Computer Graphics and Interactive Techniques* (USA, 1997), SIGGRAPH ’97, ACM Press/Addison-Wesley Publishing Co., p. 407–414. URL: <https://doi.org/10.1145/258734.258893>. 3

[LLKY19] LI X., LIU S., KAUTZ J., YANG M.: Learning linear transformations for fast image and video style transfer. In *Proceedings - 2019 IEEE/CVF Conference on Computer Vision and Pattern Recognition, CVPR 2019* (June 2019), pp. 3804–3812. [doi:10.1109/CVPR.2019.00393](https://doi.org/10.1109/CVPR.2019.00393). 3

[LWA\*12] LANG M., WANG O., AYDIN T., SMOLIC A., GROSS M.: Practical temporal consistency for image-based graphics applications. *ACM Trans. Graph.* 31, 4 (jul 2012). [doi:10.1145/2185520.2185530](https://doi.org/10.1145/2185520.2185530). 2

[LZH\*20] LIU L., ZHANG J., HE R., LIU Y., WANG Y., TAI Y., LUO D., WANG C., LI J., HUANG F.: Learning by analogy: Reliable supervision from transformations for unsupervised optical flow estimation. In *Computer Vision and Pattern Recognition (CVPR)* (2020), pp. 6488–6497. [doi:10.1109/CVPR42600.2020.00652](https://doi.org/10.1109/CVPR42600.2020.00652). 3, 5, 7

[MIH\*16] MAYER N., ILG E., HÄUSSER P., FISCHER P., CREMERS D., DOSOVITSKIY A., BROX T.: A large dataset to train convolutional networks for disparity, optical flow, and scene flow estimation. In *Computer Vision and Pattern Recognition (CVPR)* (2016), pp. 4040–4048. [doi:10.1109/CVPR.2016.438](https://doi.org/10.1109/CVPR.2016.438). 6

[Nik18] NIKLAUS S.: pytorch-pwc: a reimplementation of pwc-net in pytorch that matches the official caffe version, 2018. URL: <https://github.com/sniklaus/pytorch-pwc>. 6

[Pex] PEXELS: Pexels. URL: <https://www.pexels.com/>. 7, 8

[PGM\*19] PASZKE A., GROSS S., MASSA F., LERER A., BRADBURY J., CHANAN G., KILLEEN T., LIN Z., GIMELSHEN N., ANTIGA L., DESMAISON A., KOPF A., YANG E., DEVITO Z., RAISON M., TEJANI A., CHILAMKURTHY S., STEINER B., FANG L., BAI J., CHINTALA S.: Pytorch: An imperative style, high-performance deep learning library. In *Advances in Neural Information Processing Systems (NIPS)* (2019), pp. 8024–8035. URL: <https://proceedings.neurips.cc/paper/2019/file/bdbca288fee7f92f2bfa9f7012727740-Paper.pdf>. 6

[PP19] PUY G., PÉREZ P.: A flexible convolutional solver for fast style transfers. In *2019 IEEE/CVF Conference on Computer Vision and Pattern Recognition (CVPR)* (2019), pp. 8955–8964. [doi:10.1109/CVPR.2019.00917](https://doi.org/10.1109/CVPR.2019.00917). 3, 4

[PPTM\*16] PERAZZI F., PONT-TUSSET J., MCWILLIAMS B., VAN GOOL L., GROSS M., SORKINE-HORNUNG A.: A benchmark dataset and evaluation methodology for video object segmentation. In *2016 IEEE Conference on Computer Vision and Pattern Recognition (CVPR)* (2016), pp. 724–732. [doi:10.1109/CVPR.2016.85](https://doi.org/10.1109/CVPR.2016.85). 7, 8

[PTPC\*17] PONT-TUSSET J., PERAZZI F., CAELLES S., ARBELAEZ P., SORKINE-HORNUNG A., GOOL L. V.: The 2017 DAVIS challenge on video object segmentation. In *CoRR* (2017). [arXiv:1704.00675](https://arxiv.org/abs/1704.00675). 8, 10

[Qia99] QIAN N.: On the momentum term in gradient descent learning algorithms. *Neural Networks* 12, 1 (1999), 145–151. [doi:https://doi.org/10.1016/S0893-6080\(98\)00116-6](https://doi.org/10.1016/S0893-6080(98)00116-6). 5

[RB17] RANJAN A., BLACK M. J.: Optical flow estimation using a spatial pyramid network. In *2017 IEEE Conference on Computer Vision and Pattern Recognition (CVPR)* (2017), pp. 2720–2729. [doi:10.1109/CVPR.2017.291](https://doi.org/10.1109/CVPR.2017.291). 5

[RBL\*22] ROMBACH R., BLATTMANN A., LORENZ D., ESSER P., OMMER B.: High-resolution image synthesis with latent diffusion models. In *Proceedings of the IEEE/CVF Conference on Computer Vision and Pattern Recognition* (2022), pp. 10684–10695. 2, 9

[RDB18] RUDER M., DOSOVITSKIY A., BROX T.: Artistic style transfer for videos and spherical images. *International Journal of Computer Vision* 126, 11 (Nov 2018), 1199–1219. [doi:10.1007/s11263-018-1089-z](https://doi.org/10.1007/s11263-018-1089-z). 3, 8

[RDN\*22] RAMESH A., DHARIWAL P., NICHOL A., CHU C., CHEN M.: Hierarchical text-conditional image generation with clip latents. *arXiv preprint arXiv:2204.06125* (2022). 9

[SHR\*22] SUN D., HERRMANN C., REDA F., RUBINSTEIN M., FLEET D. J., FREEMAN W. T.: Disentangling architecture and training for optical flow. In *ECCV* (2022). 6

[SID17] SEMMO A., ISENBERG T., DÖLLNER J.: Neural style transfer: A paradigm shift for image-based artistic rendering? In *Proceedings of the Symposium on Non-Photorealistic Animation and Rendering* (2017), NPAR '17, Association for Computing Machinery. [doi:10.1145/3092919.3092920](https://doi.org/10.1145/3092919.3092920). 1

[SST\*19] SHEKHAR S., SEMMO A., TRAPP M., TURSUN O., PASEWALDT S., MYSZKOWSKI K., DÖLLNER J.: Consistent Filtering of Videos and Dense Light-Fields Without Optic-Flow. In *Vision, Modeling and Visualization* (2019), Schulz H.-J., Teschner M., Wimmer M., (Eds.). [doi:10.2312/vmv.20191326](https://doi.org/10.2312/vmv.20191326). 2, 3, 4, 10

[SVH\*21] SUN D., VLASIC D., HERRMANN C., JAMPANI V., KRAININ M., CHANG H., ZABIH R., FREEMAN W. T., LIU C.: Autoflow: Learning a better training set for optical flow. In *2021 IEEE/CVF Conference on Computer Vision and Pattern Recognition (CVPR)* (2021), pp. 10088–10097. [doi:10.1109/CVPR46437.2021.00996](https://doi.org/10.1109/CVPR46437.2021.00996). 6

[SYLK18] SUN D., YANG X., LIU M.-Y., KAUTZ J.: PWC-Net: CNNs for optical flow using pyramid, warping, and cost volume. In *Computer Vision and Pattern Recognition (CVPR)* (2018), pp. 8934–8943. [doi:10.1109/CVPR.2018.00931](https://doi.org/10.1109/CVPR.2018.00931). 3, 5, 6, 7, 8, 10

[TD20] TEED Z., DENG J.: Raft: Recurrent all-pairs field transforms for optical flow. In *Computer Vision – ECCV 2020* (2020), Vedaldi A., Bischof H., Brox T., Frahm J.-M., (Eds.), pp. 402–419. [doi:10.1007/978-3-030-58536-5\\_24](https://doi.org/10.1007/978-3-030-58536-5_24). 2, 3, 5, 8, 9, 10

[TDKP21] THIMONIER H., DESPOIS J., KIPS R., PERROT M.: Learning long term style preserving blind video temporal consistency. In *2021 IEEE International Conference on Multimedia and Expo (ICME)* (2021), IEEE, pp. 1–6. 1, 2, 3

[TFK\*20] TEXLER O., FUTSCHIK D., KUČERA M., JAMRIŠKA O., SOCHOROVÁ V., CHAI M., TULYAKOV S., SÝKORA D.: Interactive video stylization using few-shot patch-based training. *ACM Trans. Graph.* 39, 4 (2020). [doi:10.1145/3386569.3392453](https://doi.org/10.1145/3386569.3392453). 1, 4

[Vid] VIDEVO: Videvo. URL: <https://www.videvo.net/>. 7, 8

[WOG06] WINNEMÖLLER H., OLSEN S. C., GOOCH B.: Real-time video abstraction. *ACM Trans. Graph.* 25, 3 (jul 2006), 1221–1226. [doi:10.1145/1141911.1142018](https://doi.org/10.1145/1141911.1142018). 3

[YCC17] YAO C.-H., CHANG C.-Y., CHIEN S.-Y.: Occlusion-aware video temporal consistency. In *Proceedings of the 25th ACM International Conference on Multimedia* (New York, NY, USA, 2017), MM '17, Association for Computing Machinery, p. 777–785. URL: <https://doi.org/10.1145/3123266.3123363>, [doi:10.1145/3123266.3123363](https://doi.org/10.1145/3123266.3123363). 1, 2, 3

[YR19] YANG G., RAMANAN D.: *Volumetric Correspondence Networks for Optical Flow*. Curran Associates Inc., Red Hook, NY, USA, 2019. URL: <https://dl.acm.org/doi/pdf/10.5555/3454287.3454359>. 5, 6

[ZGWX05] ZHU S.-C., GUO C.-E., WANG Y., XU Z.: What are textons? *International Journal of Computer Vision* 62, 1 (2005), 121–143. 5

[ZPIE17] ZHU J.-Y., PARK T., ISOLA P., EFROS A. A.: Unpaired image-to-image translation using cycle-consistent adversarial networks. In *2017 IEEE International Conference on Computer Vision (ICCV)* (2017), pp. 2242–2251. [doi:10.1109/ICCV.2017.244](https://doi.org/10.1109/ICCV.2017.244). 7, 11